

# Crossed Andreev reflection in superconducting graphene spin-valves: Spin-switch effect

Jacob Linder,<sup>1</sup> Malek Zareyan,<sup>2</sup> and Asle Sudbø<sup>1</sup>

<sup>1</sup>*Department of Physics, Norwegian University of Science and Technology, N-7491 Trondheim, Norway*

<sup>2</sup>*Institute for Advanced Studies in Basic Sciences, 45195-1159, Zanjan, Iran*

(Dated: Received February 3, 2022)

We consider the non-local quantum transport properties of a graphene superconducting spin-valve. It is shown that one may create a spin-switch effect between perfect elastic co-tunneling (CT) and perfect crossed Andreev-reflection (CAR) for all bias voltages in the low-energy regime by reversing the magnetization direction in one of the ferromagnetic layers. This opportunity arises due the possibility of tuning the local Fermi-level in graphene to values equivalent to a weak, magnetic exchange splitting, thus reducing the Fermi surface for minority spins to a single point and rendering graphene to be half-metallic. Such an effect is not attainable in a conventional metallic spin-valve setup, where the contributions from CT and CAR tend to cancel each other and noise-measurements are necessary to distinguish these processes.

PACS numbers: 74.25.Fy, 74.45.+c, 74.50.+r, 74.62.-c

## I. INTRODUCTION

Quantum entanglement<sup>1</sup> describes a scenario where the quantum states of two objects separated in space are strongly correlated. These correlations can be exploited in emerging technologies such as quantum computing, should one be able to spatially separate the entangled objects without destroying the correlations. In a broader context, quantum entanglement could prove to be of practical importance in the fields of spintronics<sup>2</sup> and information cryptography<sup>3</sup>. It also holds a considerable interest from a purely fundamental physics point of view, prompting some of the more philosophically inclined discussions related to quantum theory and causality.

Superconductors have been proposed as natural sources for entangled electrons<sup>4,5</sup>, as Cooper pairs consist of two electrons that are both spin and momentum-entangled. The Cooper pair can be spatially deformed by means of the crossed Andreev reflection (CAR) process in superconducting heterostructures. In this scenario, an electron and hole excitation are two separate metallic leads are coupled by means of Andreev scattering processes at two spatially distinct interfaces. Unfortunately, the signatures of CAR are often completely masked by a competing process known as elastic co-tunneling (CT) which occur in the same type of heterostructures. In fact, the conductances stemming from CT and CAR may cancel each other completely<sup>6</sup>, thus necessitating the usage of noise-measurements to find fingerprints of the CAR process in such superconducting heterostructures.

Recently, graphene<sup>7</sup> has been studied as a possible arena for CAR-processes. In Ref.<sup>8</sup>, it was shown how a three-terminal graphene sheet containing *n*-doped, *p*-doped, and superconducting regions could be constructed to produce perfect CAR for one particular resonant bias voltage. Also, the signatures of the CAR process in the noise-correlations of a similar device were studied in Ref.<sup>9</sup>. However, the role played by the spin degree of freedom in graphene devices probing non-local transport has not been addressed so far. This is a crucial point since it might be possible to manipulate the spin-properties of the system to interact with the spin-singlet symmetry of the Cooper pair in a fashion favoring CAR.

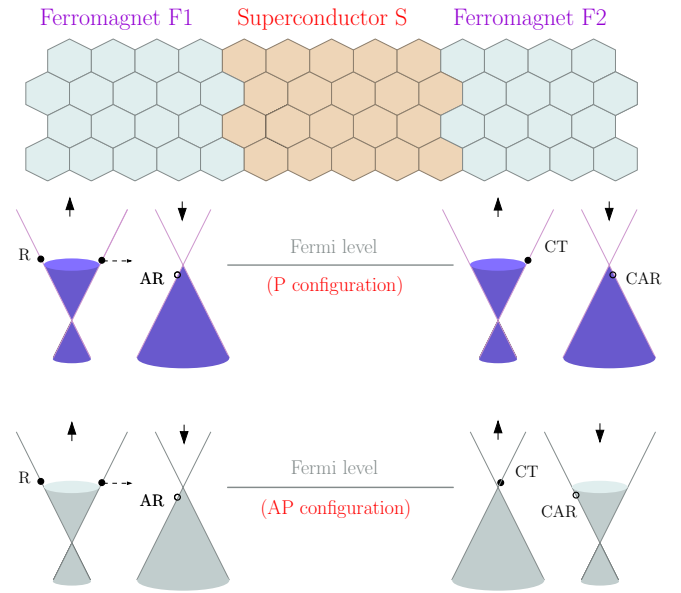


FIG. 1: (color online) Proposed experimental setup for the spin switch effect between crossed Andreev reflection and elastic co-tunneling. Ferromagnetism and superconductivity are induced by the proximity effect to a host material. The induced exchange fields in the non-superconducting graphene regions are oriented either parallel or antiparallel with respect to each other. In the parallel alignment, the density of states vanishes for both normal Andreev reflection and crossed Andreev reflection processes, such that only elastic-co-tunneling contributes to non-local transport. In the anti-parallel alignment, the density of states vanishes for both normal Andreev reflection and elastic co-tunneling, leaving only crossed Andreev reflection as the non-local transport channel.

In this paper, we show that precisely such an opportunity exists – it is possible to obtain a spin-switch effect between virtually perfect CAR and perfect CT in a superconducting graphene spin valve. In contrast to Ref.<sup>8</sup>, this effect is seen for all bias voltages in the low-energy regime rather than just at one particular applied voltage difference. The key observation is that the possibility of tuning the local Fermi-level

to values equivalent to a weak, magnetic exchange splitting in graphene renders both the usual Andreev reflection process and CT impossible. In contrast, this opportunity does not exist in conventional conductors where the Fermi energy is large and of order  $\mathcal{O}(\text{eV})$ . We show that graphene spin valves provide a possibility for a unique combination of non-local Andreev reflection and spin-dependent Klein tunneling<sup>10</sup>. Our model is shown in Fig. 1, where ferromagnetism and superconductivity are assumed to be induced by means of the proximity effect<sup>11,12</sup> to leads with the desired properties. A similar setup was considered in Ref.<sup>13</sup>, where the magnetoresistance of the system was studied.

We organize this work as follows. In Sec. II, we establish the theoretical framework which will be used to obtain the results. In Sec. III, we present our main findings for the non-local conductance in the graphene superconducting spin-valve with a belonging discussion of them. Finally, we summarize in Sec. IV.

## II. THEORY

We consider a ballistic, two-dimensional graphene structure as shown in Fig. 1. In the left ferromagnetic region  $x < 0$ , the exchange field is  $\mathbf{h} = h_0 \mathbf{z}$ , while it is  $\mathbf{h} = \pm h_0 \mathbf{z}$  in the right ferromagnetic region  $x > L$ . In the superconducting region  $0 < x < L$ , the order parameter is taken to be constant with a real gauge  $\Delta = \Delta_0$ . To proceed analytically, we make the usual approximation of a step-function behavior at the interfaces for all energy scales, i.e. the chemical potentials  $\{\mu_F, \mu_S\}$ , the exchange field  $h_0$ , and superconducting gap  $\Delta_0$ . This assumption is expected to be good when there is a substantial Fermi-vector mismatch between the F and S regions, as in the present case. To make contact with the experimentally relevant situation, we assume a heavily doped S region satisfying  $\mu_S \gg \mu_F$ .

We use the Dirac-Bogoliubov de Gennes equations first employed in Ref.<sup>14</sup>. For quasiparticles with spin  $\sigma$ , one obtains in an F|S graphene junction:<sup>15,16,17,18,19</sup>

$$\begin{pmatrix} \hat{H}_\sigma(x) & \sigma \Delta(x) \hat{1} \\ \sigma \Delta^*(x) \hat{1} & -\hat{H}_{-\sigma}(x) \end{pmatrix} \begin{pmatrix} u^\sigma \\ v^{-\sigma} \end{pmatrix} = \varepsilon \begin{pmatrix} u^\sigma \\ v^{-\sigma} \end{pmatrix}, \quad (1)$$

where

$$\hat{H}_\sigma(x) = v_F \mathbf{p} \cdot \hat{\boldsymbol{\sigma}} - [\mu(x) + \sigma h(x)] \hat{1} \quad (2)$$

and  $\hat{1}$  denotes a  $2 \times 2$  matrix. Here, we have made use of the valley degeneracy and  $\mathbf{p}$  is the momentum vector in the graphene plane while  $\hat{\boldsymbol{\sigma}}$  is the vector of Pauli matrices in the pseudospin space representing the two A, B sublattices of graphene hexagonal structure. The superconducting order parameter  $\Delta(x)$  couples electron- and hole-excitations in the two valleys ( $\mp$ ) located at the two inequivalent corners of the hexagonal Brillouin zone. The  $u^\sigma$  spinor describes the electron-like part of the total wavefunction

$$\psi^\sigma = (u^\sigma, v^{-\sigma})^T, \quad (3)$$

and in this case reads

$$u^\sigma = (\psi_{A,+}^\sigma, \psi_{B,+}^\sigma)^T \quad (4)$$

while  $v^{-\sigma} = \mathcal{T} u^\sigma$ . Here,  $^T$  denotes the transpose while  $\mathcal{T}$  is the time-reversal operator.

From Eq. (1), one may now construct the quasiparticle wavefunctions that participate in the scattering processes<sup>20</sup>. We consider positive excitation energies  $\varepsilon \geq 0$  with incoming electrons of  $n$ -type, i.e. from the conduction band  $\varepsilon = v_F |\mathbf{p}| - \mu_F$  (we set  $v_F = 1$  from now on). The incoming electron from the left ferromagnet may either be reflected normally or Andreev-reflection (AR). In the latter process, it tunnels into the superconductor with another electron situated at  $(-\varepsilon)$ , leaving behind a hole excitation with energy  $\varepsilon$ . The scattering coefficients for these two processes are  $r_e$  and  $r_h$ , respectively, and the total wavefunction may thus be written as:

$$\begin{aligned} \psi_L = & \begin{pmatrix} 1 \\ e^{i\theta} \\ 0 \\ 0 \end{pmatrix} e^{ip_e^\sigma \cos \theta x} + r_e \begin{pmatrix} 1 \\ -e^{-i\theta} \\ 0 \\ 0 \end{pmatrix} e^{-ip_e^\sigma \cos \theta x} \\ & + r_h \begin{pmatrix} 0 \\ 0 \\ 1 \\ e^{-i\theta_A^\sigma} \end{pmatrix} e^{-ip_h^\sigma \cos \theta_A^\sigma x}, \end{aligned} \quad (5)$$

where we have defined the wavevectors

$$p_e^\sigma = \varepsilon + \mu_F + \sigma h_0, \quad p_h^\sigma = \varepsilon - \mu_F + \sigma h_0. \quad (6)$$

We have omitted a common factor  $e^{ip_y y}$  for all wavefunctions. Similarly, assuming that the charge carriers in the right ferromagnetic region are also of the  $n$ -type, we obtain:

$$\begin{aligned} \psi_R = & t_e \begin{pmatrix} 1 \\ e^{i\theta} \\ 0 \\ 0 \end{pmatrix} e^{ip_e^\pm \cos \theta_N^\pm x} \\ & + t_h \begin{pmatrix} 0 \\ 0 \\ 1 \\ e^{-i\theta_A^\pm} \end{pmatrix} e^{-ip_h^\pm \cos \theta_A^\pm x}. \end{aligned} \quad (7)$$

It should be noted that the AR hole is generated in the conduction band if  $\varepsilon - \mu_F - \sigma h_0 > 0$  (retro-AR), whereas it is generated in the valence band otherwise (specular-AR). The  $\pm$  sign above refers to parallel/antiparallel (P/AP) magnetization configuration.

We assume that the superconducting region is heavily doped,  $\mu_S \gg \mu_F + h_0$ , which causes the propagating quasiparticles to travel along the  $x$ -axis since the scattering angle in the superconductor satisfies  $\theta_S \rightarrow 0$ . We obtain the following wavefunction ( $\lambda = \pm 1$ ):

$$\Psi_S = \sum_{\lambda, \pm} l_\lambda^\pm \begin{pmatrix} e^{i\lambda\beta} \\ \pm e^{i\lambda\beta} \\ 1 \\ \pm 1 \end{pmatrix} e^{\pm(i\mu_S - \lambda\kappa)x}, \quad (8)$$

where  $\kappa = \sqrt{\Delta_0^2 - \varepsilon^2}$  while

$$\beta = \text{acos}(\varepsilon/\Delta_0) \quad (9)$$

for subgap energies  $|\varepsilon| < \Delta_0$  and

$$\beta = -i \text{acosh}(\varepsilon/\Delta_0) \quad (10)$$

for supergap energies  $|\varepsilon| > \Delta_0$ .

It is important to consider carefully the scattering angles in the problem. Since we assume translational invariance in the  $y$ -direction, the  $y$ -component of the momentum is conserved. This gives us

$$p_e^\sigma \sin \theta = p_h^\sigma \sin \theta_A^\sigma = p_e^{\pm\sigma} \sin \theta_N^{\pm\sigma}. \quad (11)$$

It is clear that the angle of transmission for the electrons in the right ferromagnet is equal to the angle of incidence when the magnetizations are P, i.e.  $\theta_N^\sigma = \theta$ . Also, one infers that there exists a critical angle above which the scattered waves become evanescent, i.e. decaying exponentially. This may be seen by observing that the scattering angles exceed  $\pi/2$  (thus becoming imaginary) above a certain angle of incidence  $\theta$ . For instance, the AR wave in the left ferromagnetic region becomes evanescent for angles of incidence  $\theta > \theta_{AR}^\sigma$ , where the critical angle  $\theta = \theta_{AR}^\sigma$  is obtained by setting  $\theta_A^\sigma = \pi/2$  in the equation

$$p_e^\sigma \sin \theta = p_h^\sigma \sin \theta_A^\sigma, \quad (12)$$

expressing conservation of momentum perpendicular to the interface. One finds that:

$$\theta_{AR}^\sigma \equiv |\text{asin}[(\varepsilon - \mu_F + \sigma h_0)/(\varepsilon + \mu_F + \sigma h_0)]|. \quad (13)$$

Thus, AR waves in the regime  $\theta > |\theta_c^\sigma|$  do not contribute to any transport of charge. A similar argument can be made for the transmitted electron wave-function in the right ferromagnetic region, corresponding to the CT process, where the critical angle for this process becomes

$$\theta_{CT}^\sigma \equiv |\text{asin}[(\varepsilon + \mu_F \pm \sigma h_0)/(\varepsilon + \mu_F + \sigma h_0)]|. \quad (14)$$

In the P configuration, the CT process thus always contributes to the transport of charge. Finally, the contribution to transport of charge from CAR comes from the hole-wave function in the right ferromagnetic region, which becomes evanescent for angles of incidence above the critical angle

$$\theta_{CAR}^\sigma > |\text{asin}[(\varepsilon - \mu_F \pm \sigma h_0)/(\varepsilon + \mu_F + \sigma h_0)]|. \quad (15)$$

In the P configuration, this criteria is the same as the vanishing of local AR expressed by Eq. (13).

### III. RESULTS AND DISCUSSION

Intuitively, one might expect that the most interesting phenomena occur when the exchange field  $h_0$  is comparable in magnitude to the chemical potential  $\mu_F$ . If  $\mu_F \gg h_0$ , the effect of the exchange field should be minor and the AR is never

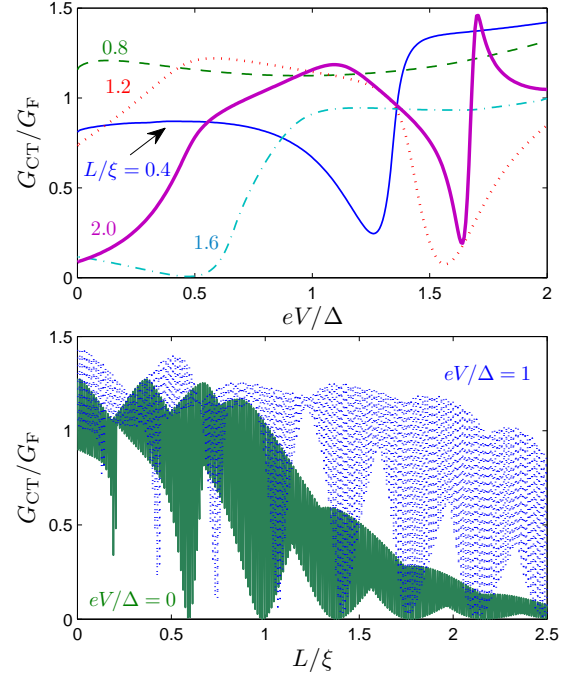


FIG. 2: (color online) Plot of the conductance for CT processes  $G_{CT}/G_F$  versus bias voltage in the upper panel and versus length of the S region in the lower panel. Here, we consider the P alignment and  $\mu_F = h_0$  such that  $G_{CAR} \rightarrow 0$ .

specular. In contrast, the situation becomes quite fascinating when we consider the case  $\mu_F = h_0$  under the assumption of a doped situation  $\mu_F \gg (\varepsilon, \Delta_0)$ . First of all, the incoming quasiparticles from the left ferromagnetic region are completely dominated by the majority spin carriers  $\sigma = \uparrow$ , since the density of states (DOS) for  $\sigma = \downarrow$  electrons vanishes at the Fermi level. Since  $\mu_F = h_0$ , the AR process is suppressed for all incoming waves as  $\theta_{AR}^\uparrow \rightarrow 0$ . We now show how the fate of the cross-conductance in the right ferromagnetic region depends crucially on whether the magnetization configuration is P or AP. In the P configuration, we see that  $\theta_{CAR}^\uparrow \rightarrow 0$ , which means that the transport is purely governed by the CT process. In the AP configuration, we see that  $\theta_{CT}^\uparrow \rightarrow 0$ , which means that the transport is mediated purely by the CAR process. This suggests a remarkable spin-switch effect – by reversing the direction of the field in the right ferromagnet, one obtains an abrupt change from pure CT to pure CAR processes mediating the transport of charge. In each case, there is no local AR in the left ferromagnetic region. In the standard metallic case, the distinct signatures for the CT and CAR contributions are masked by each other, and it becomes necessary to resort to noise-measurements in order to say something about the contribution from each process. In the present scenario, we have showed how it is possible to separate the two contributions directly by a simple spin-switch effect which is commonly employed in experimental work on F|S heterostructures.

Let us now evaluate the conductance in the P and AP con-

figuration quantitatively by using

$$G_{\text{CAR}}/G_F = \sum_{\sigma} (G^{\sigma}/G_F) \int_{-\pi/2}^{\pi/2} d\theta \cos \theta |t_h|^2, \quad (16)$$

where we have introduced

$$G^{\sigma} = e^2 N^{\sigma}(eV)/\pi \quad (17)$$

as the spin- $\sigma$  normal-state conductance that takes into account the valley degeneracy, in addition to

$$G_F = G^+ + G^-. \quad (18)$$

The density of states is determined by

$$N^{\sigma}(\varepsilon) = |\varepsilon + \mu_F + \sigma h|W/(\pi v_F), \quad (19)$$

where  $W$  is the width of the junction. The expression for  $G_{\text{CT}}$  is obtained by replacing  $t_h$  with  $t_e$  in Eq. (16). Since we here consider the case  $\mu_F = h_0$  and  $h_0 \gg (\varepsilon, \Delta_0)$ , the formulas for the  $G_{\text{CAR}}$  and  $G_{\text{CT}}$  may be simplified since  $G_- \ll G_+$ . Also, since the DOS vanishes for minority spins for the injected electrons, only  $\sigma = \uparrow$  contributes for incoming electrons. The crucial point here is that in the P alignment,  $G_{\text{CAR}} \rightarrow 0$  and  $G_{\text{CT}} \neq 0$  such that

$$|r_e|^2 + |t_e|^2 = 1, \quad (20)$$

while in the AP alignment  $G_{\text{CAR}} \neq 0$  and  $G_{\text{CT}} \rightarrow 0$  such that

$$|r_e|^2 + |t_h|^2 = 1. \quad (21)$$

In the actual numerical calculations, we use  $h_0/\Delta_0 = 50$  and  $\mu_S/\Delta_0 = 500$ . Assuming a value of  $\Delta_0 = 0.1$  meV for the proximity-induced gap, this corresponds to an exchange splitting of  $h_0 = 5$  meV in the F regions and a doping level  $\mu_S = 50$  meV in the S region, which should be experimentally feasible<sup>21</sup> and well within the range of the validity for the linear dispersion relation in graphene. In Fig. 2, we plot the cross-conductance  $G_{\text{CT}}/G_F$  in the P alignment both as a function of bias voltage and width of the S region. The same thing is done for  $G_{\text{CAR}}/G_F$  in the AP alignment in Fig. 3. In both cases, the magnitude of the conductance varies strongly when considering different widths  $L$  due to the fast oscillations which pertain to the formation of resonant transmission levels inside the superconductor. Also, it is seen that while the CT process is favored for short junctions  $L/\xi \ll 1$ , the CAR process is suppressed in this regime in favor of normal reflection. Upon increasing the junction width, the CT conductance drops while the CAR conductance peaks at widths  $L \sim \xi$ . The remarkable aspect is that it is possible to switch between these two scenarios of exclusive CT and exclusive CAR simply by reversing the direction of magnetization in one of the ferromagnetic layers.

In order to obtain analytical results, we have assumed that the Coulomb interaction and charge inhomogeneities may be neglected. It would be challenging to obtain a truly homogeneous chemical potential in a graphene sheet, and electron-hole puddles appear to be an intrinsic feature of graphene

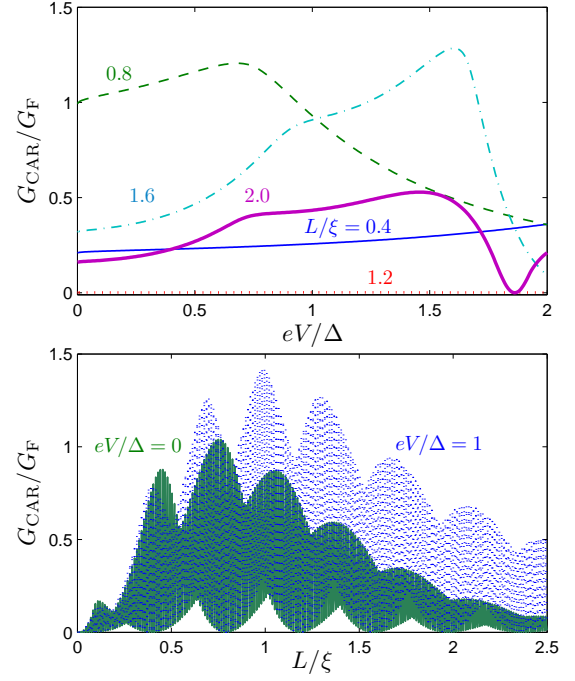


FIG. 3: (color online) Plot of the conductance for CAR processes  $G_{\text{CAR}}/G_F$  versus bias voltage in the upper panel and versus length of the S region in the lower panel. Here, we consider the AP alignment and  $\mu_F = h_0$  such that  $G_{\text{CT}} \rightarrow 0$ .

sheets<sup>22</sup>. Moreover, it has been speculated that such charge inhomogeneities may play an important role with regard to limiting the transport characteristics of graphene<sup>23</sup> near the Dirac points. However, for our purposes this is actually beneficial – it is precisely the suppression of charge and spin transport at Fermi level for the Andreev reflection and co-tunneling process which renders possible the spin-switch effect. Therefore, we do not expect that the inclusion of charge inhomogeneities should alter our results qualitatively. Finally, we note that since the spin of the charge-carriers in each of the non-superconducting graphene sheets are practically speaking fixed due to the vanishing DOS for minority spins, the spin-switch effect for CAR and EC predicted in this paper can not be directly related to entanglement. Nevertheless, it constitutes a clear non-local signal for quantum transport which can be probed experimentally, and should be helpful in identifying clear-signatures of the mesoscopic CAR phenomenon.

#### IV. SUMMARY

To summarize, we have considered non-local quantum transport in a graphene superconducting spin-valve. We have shown how one may create a spin-switch effect between perfect elastic co-tunneling and perfect crossed Andreev-reflection for all applied bias voltages by reversing the magnetization direction in one of the ferromagnetic layers. The basic mechanism behind this effect is that the local Fermi-level in graphene may be tuned so that the Fermi surface for minority

spins reduces to a single point in the presence of a weak, magnetic exchange splitting. This is very distinct from the equivalent spin valve structures in conventional metallic systems, where noise-measurements are required to clearly distinguish between these processes.

### Acknowledgments

J.L. and A.S. were supported by the Norwegian Research Council Grant Nos. 158518/431, 158547/431, (NANOMAT),

and 167498/V30 (STORFORSK).

- 
- <sup>1</sup> J. M. Raimond, M. Brune, and S. Haroche, *Rev. Mod. Phys.* **73**, 565 (2001); L. Amico, R. Fazio, A. Osterloh, and V. Vedral, *Rev. Mod. Phys.* **80**, 517 (2008).
  - <sup>2</sup> I. Zutic, J. Fabian, and S. Das Sarma, *Rev. Mod. Phys.* **76**, 323 (2004).
  - <sup>3</sup> A. Galindo and M. A. Martin-Delgado, *Rev. Mod. Phys.* **74**, 347 (2002).
  - <sup>4</sup> G. Burkard, D. Loss, and E. V. Sukhorukov, *Phys. Rev. B* **61**, R16 303 (2000).
  - <sup>5</sup> P. Recher, E. V. Sukhorukov, and D. Loss, *Phys. Rev. B* **63**, 165314 (2001).
  - <sup>6</sup> G. Falci, D. Feinberg, F.W.J. Hekking, *Europhys. Lett.* **54**, 255 (2001).
  - <sup>7</sup> K. S. Novoselov, A.K. Geim, S.V. Morozov, D. Jiang, Y. Zhang, S.V. Dubonos, I.V. Grigorieva, and A.A. Firsov, *Science* **306**, 666 (2004).
  - <sup>8</sup> J. Cayssol, *Phys. Rev. Lett.* **1100**, 147001 (2008).
  - <sup>9</sup> C. Benjamin and J. K. Pachos, arXiv:0802.3181.
  - <sup>10</sup> M. I. Katsnelson, K. S. Novoselov, and A. K. Geim, *Nature Phys.* **2**, 620 (2006).
  - <sup>11</sup> E. W. Hill *et al.*, *IEEE Trans. Magn.* **42**, 2694 (2006); N. Tombros *et al.*, *Nature* **448**, 571 (2007); M. Ohishi *et al.*, *Jpn. J. Appl. Phys.* **46** L605 (2007).
  - <sup>12</sup> H. B. Heersche, P. Jarillo-Herrero, J. B. Oostinga, L. M. K. Vandersypen, and A. F. Morpurgo, *Nature (London)* **446**, 56 (2006); A. Shailos, W. Nativel, A. Kasumov, C. Collet, M. Ferrier, S. Gueron, R. Deblock, and H. Bouchiat, *Europhys. Lett.* **79**, 57008 (2007).
  - <sup>13</sup> C. Bai, Y. Yang, and X. Zhang, *Appl. Phys. Lett.* **92**, 102513 (2008).
  - <sup>14</sup> C. W. J. Beenakker, *Phys. Rev. Lett.* **97**, 067007 (2006).
  - <sup>15</sup> J. Linder, T. Yokoyama, D. Huertas-Hernando, and A. Sudbø, *Phys. Rev. Lett.* **100**, 187004 (2008).
  - <sup>16</sup> A. G. Moghaddam and M. Zareyan, *Phys. Rev. B* **78**, 115413 (2008).
  - <sup>17</sup> M. Zareyan, H. Mohammadpour, and A. G. Moghaddam, *Phys. Rev. B* **78**, 193406 (2008).
  - <sup>18</sup> Y. Asano, T. Yoshida, Y. Tanaka, and A. A. Golubov, *Phys. Rev. B* **78**, 014514 (2008).
  - <sup>19</sup> Q. Zhang, D. Fu, B. Wang, R. Zhang, and D. Y. Xing, *Phys. Rev. Lett.* **101**, 047005 (2008).
  - <sup>20</sup> J. Linder and A. Sudbø, *Phys. Rev. B* **77**, 064507 (2008); J. Linder and A. Sudbø, *Phys. Rev. Lett.* **99**, 147001 (2007).
  - <sup>21</sup> H. Haugen, D. Huertas-Hernando, and A. Brataas, *Phys. Rev. B* **77**, 115406 (2008).
  - <sup>22</sup> J. Martin, N. Akerman, G. Ulbricht, T. Lohmann, J. H. Smet, K. von Klitzing, and A. Yacoby, *Nature Physics* **4**, 144 (2008).
  - <sup>23</sup> E.-A. Kim and A. H. Castro Neto, arXiv:0702.562.